Check for updates

Transient Analysis of Tilt Pad Journal Bearings Including Effects of Pad Flexibility and Fluid Film Temperature

R. K. Gadangi

A. B. Palazzolo

Department of Mechanical Engineering,
Texas A&M University,
College Station, TX 77843

The paper considers vibration response of spinning shafts supported by flexible tilt pad journal bearings, to large mass imbalance (blade loss). A time transient study of the tilt pad journal bearing with thermal effects and without pad deformations, and with pad deformations and without thermal effects, is performed. Influence of the inclusion of thermal effects on the journal center's orbit, the minimum film thickness, and the maximum film temperature is evaluated, and also the influence of pad deformations due to the fluid film forces on the journal center's orbit and the minimum film thickness is studied. Inclusion of thermal effects had little effect on the orbit, while the inclusion of pad deformations had considerable effect on the journal orbit and the minimum film thickness. Three cases are studied in this paper; static load without imbalance, static load with low imbalance, and static load with high imbalance.

Introduction

The purpose of this research is to study the nonlinear response of tilt pad journal bearings supported rotors when subjected to high unbalance (dynamic load). Palazzolo et al. (1989) studied the effects of blade loss in steam and gas turbines but employed Active Vibration Control. Earles and Palazzolo (1990), and Kim and Palazzolo (1993) studied the response due to small unbalance and the stability of a rotorbearing system supported by tilt pad journal bearings. Gadangi and Palazzolo (1993), studied the effects of including the steady state isoadi effects in the transient analysis of plain journal bearings, which showed that inclusion of thermal effects can be very important. They also considered the isoviscous transient analysis of tilt pad journal bearings subjected to sudden unbalance. They compared the results obtained with nonlinear analysis, liner analysis and pseudo transient analysis, and showed good agreement between the nonlinear analysis and pseudo transient analysis for the cases considered. The pseudo transient analysis treated the response as a succession of steady state responses to the time varying load. Choy et al. (1992) performed a transient analysis of an isoviscous plain journal bearing due to impulse loading. Malik and Bhargava (1992) studied the time dependent response of a short journal bearing, assuming a flexible rotor and damped pedestals. The approximate short journal model excluded temperature effects.

A diagram illustrating the principle components of a tilt pad journal bearing is shown in Fig. 1. The rotor shaft is assumed to be rigid and supported on fluid film bearings as shown in Fig. 2. The current paper compares the following three cases used in the nonlinear transient analysis of tilt pad journal bearings;

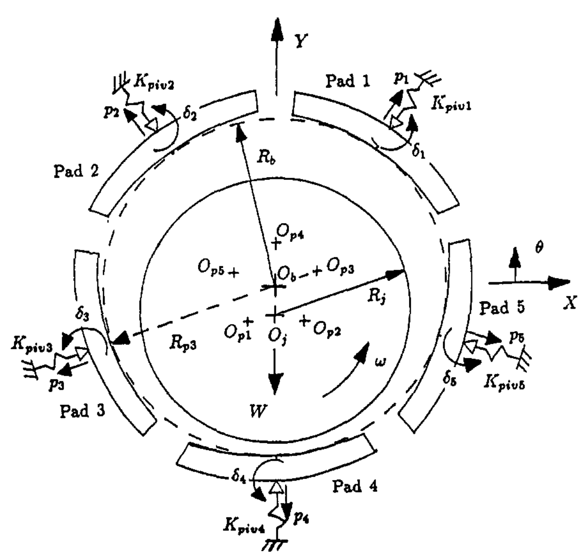

Fig. 1 Tilt pad journal bearing schematic

Contributed by the Tribology Division of THE AMERICAN SOCIETY OF MECHANICAL ENGINEERS and presented at the ASME/STLE Tribology Conference, Maui, Hawaii, October 16–19, 1994. Manuscript received by the Tribology Division March 1, 1994; revised manuscript received July 12, 1994. Paper No. 94-Trib-47. Associate Technical Editor: M. J. Braun.

Copyright © 1995 by ASME

Downloaded from http://asmedigitalcollection.asme.org/tribology/article-pdf/117/2/302/5938013/302_1.pdf?casa_token=f_wYh5kA57kAAAAA:pG4tYZoMXN_4YNElo3bpW78bwQcQHni052zna1AVq3RYmU934X418ITREIZbJKG8229tiQ by Texas A & M University user on 08 August 2023

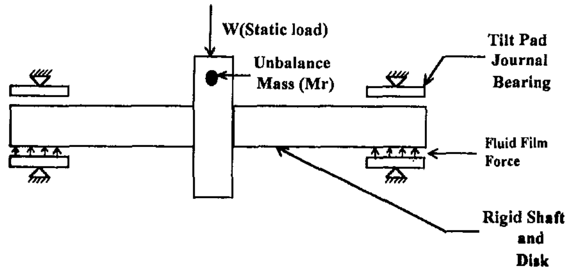

Fig. 2 Model of the rigid rotor on flexible fluid film bearings

(1) Isoviscous fluid film and rigid pads
(2) Fluid film thermal effects and rigid pads
(3) Isoviscous fluid film and flexible pads (rigid pivots)

The contributions of this paper are:

- tilt pad journal bearing nonlinear transient analysis
- variable viscosity fluid film thermal effects in the tilt pad journal bearing on the transient unbalance response orbits
- pad flexibility effects in the tilt pad journal bearing on the transient unbalance response orbits.

Theory

Reynolds Equation. Three cases of the tilt pad journal bearing analysis are studied in this paper. The isoviscous rigid pad (IVRP) case, isoviscous flexible pad (IVFP) case, and isoadi rigid pad (IARP) case. In the IVRP case the temperature of the fluid film is assumed to be at the fluid inlet temperature and the viscosity is held constant throughout the lubricant film, and the pad is assumed to be rigid (no pad deformation due to fluid film pressures). In the IARP case the shaft/journal is fixed at a constant temperature, the pad and fluid interface is considered to be insulated, the pads are rigid, and the viscosity varies throughout the lubricant film in response to the calculated temperature (ISOADI: ISOthermal (constant) shaft temperature and ADIabatic (insulated) pad-fluid film interface). The variable viscosity Reynolds equation is (Huebner, 1982);

$$\nabla \cdot (C_1 \nabla p) + (\nabla C_2) \cdot \mathbf{U} + \frac{\partial h}{\partial t} = 0 \tag{1}$$

where

$$C_1 = \int_0^h \int_0^z \frac{\zeta}{\mu}\, d\zeta\, dz - \frac{\int_0^h \zeta/\mu\, d\zeta}{\int_0^h d\zeta} \int_0^h \int_0^z \frac{1}{\mu}\, d\zeta\, dz \tag{2}$$

$$C_2 = \frac{\int_0^h \int_0^\zeta 1/\mu\, d\zeta\, dz}{\int_0^h 1/\mu\, d\zeta} \tag{3}$$

In the IVFP case the fluid film temperatures and viscosity are held constant, while the pad is allowed to deform under the application of the fluid film pressures on the pad surface. When the viscosity is held constant, Eq. (1) reduces to

$$\nabla \cdot \left(\frac{\rho h^3}{12\mu} \nabla p \right) + \nabla(\rho h) \cdot \mathbf{U} + \frac{\partial(\rho h)}{\partial t} = 0 \tag{4}$$

The fluid film thickness expressions are given by

$$h_e = C_p - x \cos\theta - y \sin\theta - (C_p - C_b)\cos(\theta - \theta_p) - \delta(R_j + t_p)\sin(\theta - \theta_p) \tag{5}$$

$$h_t = h_e + h_d \tag{6}$$

Only the radial component of the pad deformation is included in the fluid film thickness expression, the tangential component is neglected. For a rigid pad case $h_d = 0.0$.

The Reynolds equation is solved by using the functional given in Huebner, (1982). It was found that simplex 3-node finite elements (Allaire et al., 1975) were as effective as the isoparametric elements in solving Reynolds equation. The pressures obtained from Reynolds equation's solutions are integrated over the bearing area (taking into consideration the possibility of cavitation) to obtain the reaction forces. The pressure distribution is used in calculating the velocity profiles which are required in solving the Energy equation. Reynolds boundary condition is implemented at the cavitation boundary, to ensure flow continuity.

Energy Equation. The fluid film energy equation has to be solved for the *isoadi* case to find the actual viscosity distribution throughout the fluid film. The energy equation is

$$\rho c_p\, \mathbf{u} \cdot \nabla T = \nabla \cdot (k \nabla T) + \mu \left[\left(\frac{\partial u}{\partial y} \right)^2 + \left(\frac{\partial w}{\partial y} \right)^2 \right] \tag{7}$$

The Reynolds equation and energy equation are coupled through viscosity and the velocity distributions. Reynolds equation's solution gives pressures, the gradients of pressure are used to find the fluid velocity field, and these velocity distributions are included in the energy equation. The viscosity distribution is required in the evaluation of fluid pressures using variable viscosity Reynolds equation, the viscosity is

Nomenclature

- C_b = radial bearing clearance (m)
- C_p = radial pad clearance (m)
- c_p = fluid specific heat (J/kg°C)
- F_{x_f} = x-component of fluid film force (N)
- F_{y_f} = y-component of fluid film force (N)
- F_{x_u} = x-component of unbalance force (N) $= -M_R u_b \omega^2 \cos(\omega t)$
- F_{y_u} = y-component of unbalance force (N) $= -M_R u_b \omega^2 \sin(\omega t)$
- h_d = Pad deformation contribution to h_t (m)
- h_e = fluid film thickness due to journal eccentricity pad tilt angle (m)
- h_t = total fluid film thickness ($h_e + h_d$) (m)
- I_p = polar moment of inertia of a pad about the pivot (kg − m^2)
- k = thermal conductivity (W/m°C)
- M_R = Rotor Mass (kg)
- $M_{n\text{pad}}$ = sum of the moments on the nth pad (N − m)
- $n$pad = nth pad
- R_j = journal radius
- Δt = time increment (s)
- t = time (s)
- T = Temperature (°C)
- u, v, w = components of velocity vector $\mathbf{u}$ (m/s)
- u_b = unbalance eccentricity (m)
- u_p = pad deformation (m)
- x, y = cartesian coordinates
- z = cross film directions
- δ = pad tilt angle (rad)
- μ = viscosity of lubricant (N − s/m^2)
- β = viscosity coefficient (1/°C)
- ρ = density of lubricant (kg/m^3)
- θ = circumferential coordinate (rad)
- θ_p = pad pivot location (rad)
- ζ = nondimensional cross film distance
- ω = shaft speed (rad/s)
- $\dot{}$ = $(\partial/\partial t)$
- $\ddot{}$ = $(\partial^2/\partial t^2)$

Downloaded from http://asmedigitalcollection.asme.org/tribology/article-pdf/117/2/302/5938013/302_1.pdf?casa_token=f_wYh5kA57kAAAAA:pG4tYZoMXN_4YNElo3bpW78bwQcQHni052zna1AVq3RYmU934X418ITREIZbJKG8229tiQ by Texas A & M University user on 08 August 2023

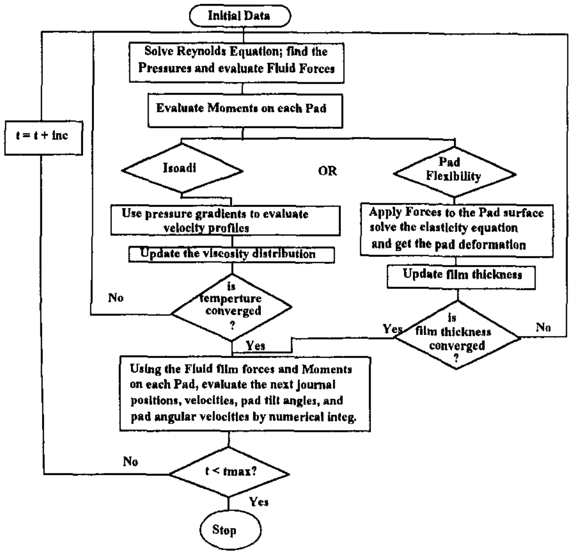

Fig. 3 Flowchart for tilt pad journal bearing analysis

updated at each instant using the new temperature field. The viscosity is assumed to follow the exponential relationship given by

$$\mu = \mu_o \, e^{-\beta(T-T_o)} \tag{8}$$

Density of the lubricant is assumed to be constant, i.e., no significant variation with temperature unlike the viscosity. Numerical oscillations arise due to the presence of the convection term on the left hand side of Eq. (7). A finite element upwinding technique is used to suppress these oscillations (Kim, 1993). The weighted residual finite element method is used to solve the energy equation by discretizing the problem domain into 4-node isoparametric elements. The weight functions employed are the upwind functions given in Christie et al. (1976). The fluid velocities obtained from Reynolds equation, are used in the energy equation to solve for updated temperatures in the fluid film. The boundary conditions used in solving this equation are:

(1) Supply temperature is prescribed at the leading edge of fluid film on each pad.

(2) Isothermal shaft temperature is prescribed at the shaft-fluid film interface.

(2) The pad-fluid film interface is insulated (adiabatic interface).

Cavitation in the energy equation is handled by assuming the presence of only air in the cavitated region. The time dependent term ($\partial T/\partial t$) is neglected so that the energy equation is solved at each time increment in a pseudo-static manner.

Elasticity Equation. Four noded isoparametric plain strain finite elements are employed to discretize the problem domain for the pad's elastic deformation. The surface nodal degrees of freedom are specified as the master degrees of freedom, and Guyan Reduction is performed to obtain a reduced (super-element) stiffness matrix $[K_{mm}]$, from which;

$$[K_{mm}]\ \{u_p\} = \{F_s\} \tag{9}$$

The boundary conditions used in solving the pad elasticity equation are;

- node at the pivot is fixed in both directions
- node just below the surface of the pad center is fixed in the transverse direction (for calculating pad deformation about the pad's current rigid body position),
- forces obtained from integrating the fluid film pressures (F_s) are resolved into x and y components and applied to the pad surface nodes as specified forces,
- the pivot is assumed to be rigid.

Table 1 Tilt pad bearing data for Fillon et al. (1992) bearing

Parameter	Symbol	Value and Units
Journal diameter	D	0.1 m
Bearing length	L	0.07 m
Radial pad clearance	C_r	$0.148e^{-3}$m
Preload	m_p	0.47
Pad thickness	d	0.02 m
Pad arc angle		75°
Offset		0.5
Lubricant viscosity	μ	0.0277 N − s/m^2
Lubricant viscosity coeff.	β	0.0341/°C
Lubricant specific heat	c_p	1951.8 J/kg°C
Lubricant thermal conductivity	k	0.149 W/m°C
Lubricant density	ρ	860 kg/m^3
Rotor speed	ω	209.44 (rad/s)
Rotor mass	M_R	1000 kg
Static load	W	20 kN

The finite element meshes are adjusted such that the nodes at the surface for the pad elasticity mesh correspond with those from the fluid film pressure mesh.

Solution Procedure. Figure 3 shows the flow chart for the time transient (nonlinear) analysis of the response of a tilt pad journal bearing. A Runge Kutta fourth-order scheme is used for numerically integrating the following equations:

$$\ddot{x} = (F_{x_f} + F_{x_u})/M_R \tag{10}$$

$$\ddot{y} = (F_{y_f} + F_{y_u} - W)/M_R \tag{11}$$

The equation of motion for the pads in the pad coordinate system is given as:

$$\ddot{\delta} = M_{n\text{pad}}/I_p \tag{12}$$

The procedure for finding the updated values at every time step is as follows:

(*a*) Select a time increment.

(*b*) Define the initial conditions on the journal and the pads ($\dot{x}(0)$, $\dot{y}(0)$, $x(0)$, $y(0)$, $\dot{\delta}_{n\text{pad}}(0)$, and $\delta_{n\text{pad}}(0)$).

(*c*) Use the finite element method to solve the variable viscosity Reynolds equation (Eq. (1)) for the pressures and velocity profiles. Integrate the pressures to get the reaction forces on the shaft and the sum of the moments on the pads

(*d*) Use the velocity profiles in solving the energy equation for temperatures.

(*e*) Update the viscosity distribution using Eq. (6).

(*f*) Repeat steps (*c*), (*d*), and (*e*) until the temperatures converge for this time step.

(*g*) Apply the fluid film forces to the pad surface nodes in the pad elasticity mesh and get the deflections

(*h*) Update the fluid film thickness h_t and repeat steps (*c*) and (*g*) until the fluid film thickness converges

(*i*) Use the Runge Kutta scheme to integrate the Eqs. (7), (8), and (9), to find the new journal center position, velocities, pad tilt angles, and pad angular velocities.

(*j*) Continue until the final time is reached.

Note that for the IVRP problem steps (*d*), (*e*), (*f*), (*g*), and (*h*) are omitted from the solution procedure. For the IARP problem steps (*g*) and (*h*) are omitted from the solution procedure. For the IVFP problem steps (*d*), (*e*), and (*f*) are neglected.

The data for the tilt pad bearing is obtained from Fillon et al. (1992), and is shown in Table 1. This tilt pad bearing is a 4-pad, load between pad bearing.

Results and Discussion

Static Equilibrium. Table 2 shows the results obtained for the tilt pad journal bearing (Table 1), for all three models subjected to an external static load of 20 kN, and with a rotor

Downloaded from http://asmedigitalcollection.asme.org/tribology/article-pdf/117/2/302/5938013/302_1.pdf?casa_token=f_wYh5kA57kAAAA:pG4tYZoMXN_4YNElo3bpW78bwQcQHni052zna1AVq3RYmU934X418iITREIZbJKG8229tiQ by Texas A & M University user on 08 August 2023

Table 2 Summary of static equilibrium positions

Model	Newton-Raphson Eccentricity		Nonlinear transient Eccentricity	
	x μm	y μm	x μm	y μm
IVRP	0.25	−84.72	0.12	−84.15
IVFP	1.35	−87.94	1.22	−87.78
IARP	0.29	−85.97	0.63	−85.14

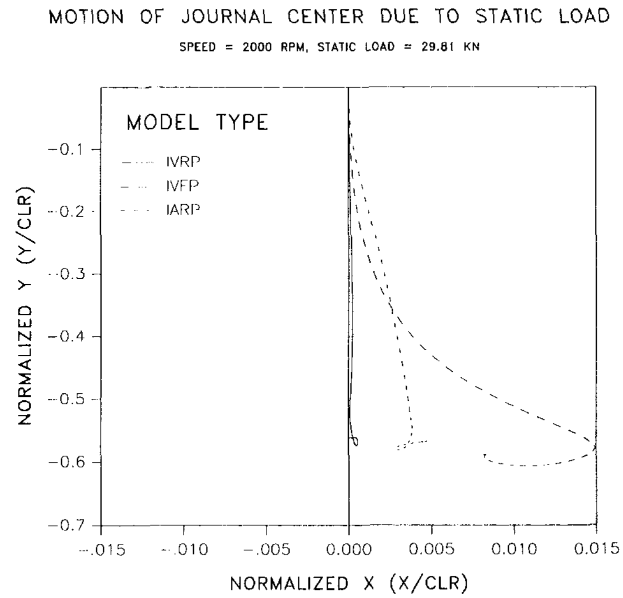

Fig. 4 Transient motion to the static equilibrium for tilt pad journal bearing

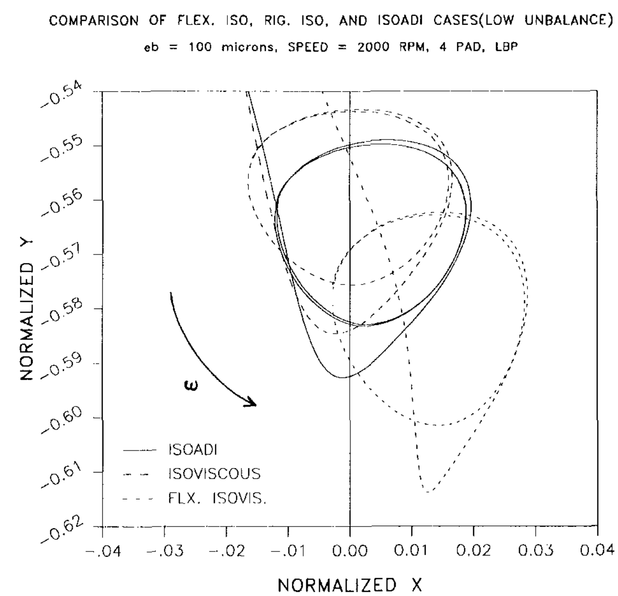

Fig. 5 Comparison of low unbalance orbits for the three models ($e_b = 100$ μ_m)

mass (M_R) of 1000 kg. The results in this table and the journal loci in Fig. 4 show that the three models have different equilibrium positions. The results obtained with transient analysis are in good agreement with the ones obtained with Newton-Raphson scheme. The Newton-Raphson scheme provides an alternate solution to the steady state static equilibrium problem by locating the journal and pad positions which yield zero residual forces and moments, i.e., fluid film forces balance the externally applied static load. The Newton-Raphson derivatives are determined numerically about the current guess of the equilibrium configuration (Kim, 1993).

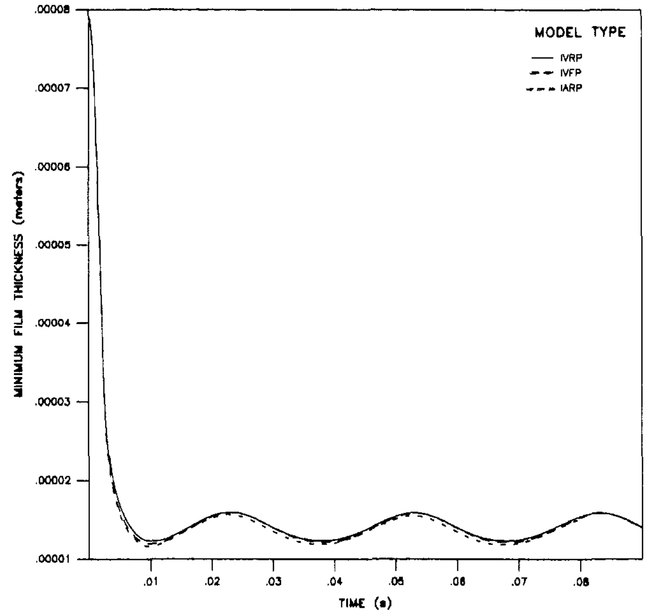

Fig. 6 Minimum film thickness variation with time on pad 3 for low unbalance case ($e_b = 100$ μm)

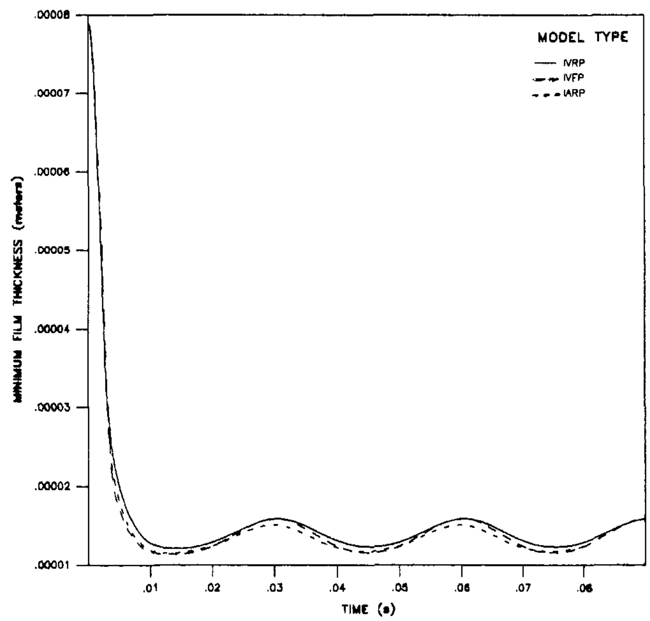

Fig. 7 Minimum film thickness variation with time on pad 4 for low unbalance case ($e_b = 100$ μ_m)

Response to Dynamic Loading

Low Unbalance Case. The low unbalance case is run with an unbalance eccentricity of 100.0 μm. The analysis is started from the center of the bearing with the unbalance. The resulting three orbits are shown in Fig. 5. The minimum film thickness variation for the two loaded pads (Pads 3 and 4) with time are shown in Figs. 6 and 7, respectively. All three models show similar pattern and magnitude for pad 3, but for the pad 4, the film thickness for the IVFP model is less than the other two models. The maximum temperature variation with time on the two loaded pads is shown in Fig. 8. The general shape

Downloaded from http://asmedigitalcollection.asme.org/tribology/article-pdf/117/2/302/5938013/302_1.pdf?casa_token=f_wYh5kA57kAAAAA:pG4tYZoMXN_4YNElo3bpW78bwQcQHni052zna1AVq3RYmU934X418ITREIZbJKG8229tiQ by Texas A & M University user on 08 August 2023

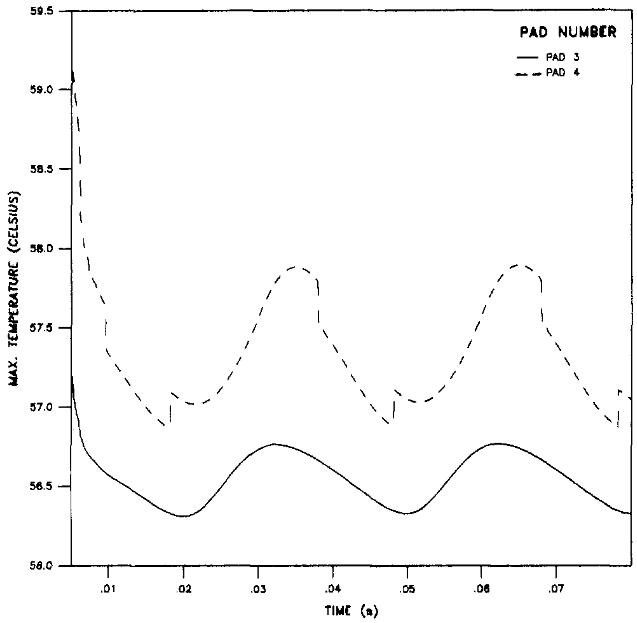

Fig. 8 Maximum film temperature variation with time for low unbalance case ($e_b = 100$ μm)

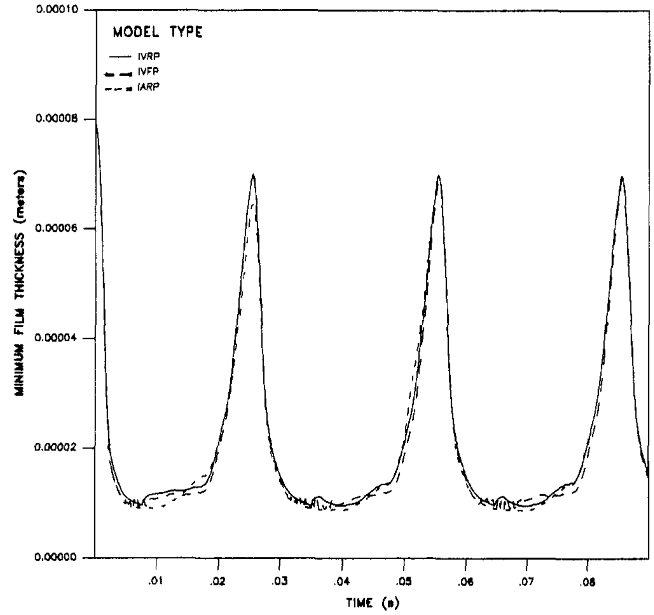

Fig. 10 Minimum film thickness variation with time on pad 3 for high unbalance case ($e_b = 570$ μm)

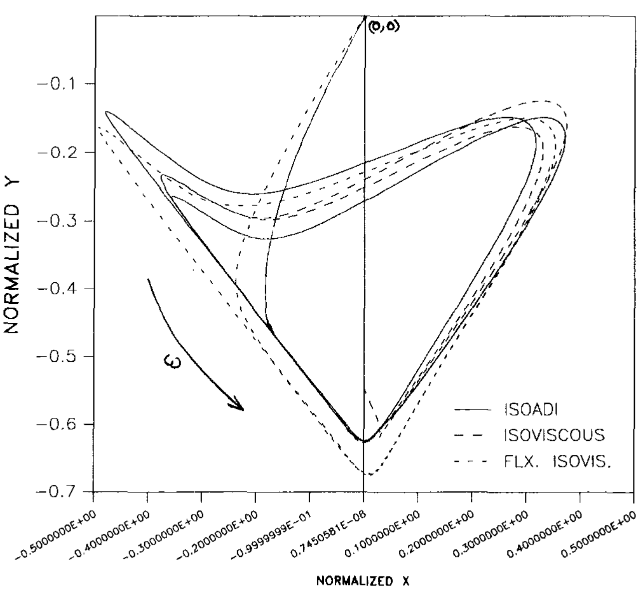

Fig. 9 Comparison of high unbalance orbits for the three models ($e_b = 570$ μ_m)

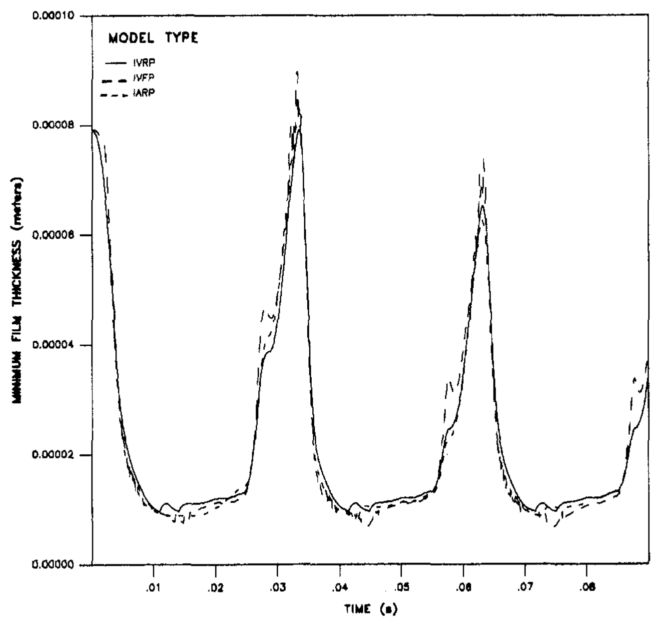

Fig. 11 Minimum film thickness variation with time on pad 4 for high unbalance case ($e_b = 570$ μ_m)

of the orbits is the same but the location of their centers of revolution is different. The minimum film thickness plots for all the three cases show a sinusoidal variation with time because of the low unbalance. The same is observed in the case of maximum film temperature for the IARP case, for the two loaded pads.

High Unbalance Case. The unbalance eccentricity used for this case is 570 μm. Figure 10 shows the journal center orbits for the three cases. The plots show that there is a significant difference between the IVFP and IVRP cases, and a smaller difference between the IVRP and IARP cases. The inclusion of pad flexibility and fluid film temperature effects is seen to have a significant influence on the unbalance response of the tilt pad journal bearing subjected to high unbalance. The minimum film thickness variation for the three models for pads 3 and 4 are shown in Figs. 9 and 10. The general shape is retained in all the three cases but the magnitude is changed. The maximum film temperature variation on pads 3 and 4 is shown in Fig. 11. The variation is erratic, but follows a periodic distribution. The responses assume a steady orbit within about three shaft revolutions.

Conclusions

A nonlinear analysis of a tilt pad journal bearing due to unbalance has been performed. The influence of pad flexibility and fluid film thermal effects have been studied. The inclusion of these effects produces a bigger orbit, implying reduction in minimum film thickness and increase in maximum temperatures. The pressures also increase with decrease in minimum

Downloaded from http://asmedigitalcollection.asme.org/tribology/article-pdf/117/2/302/5938013/302_1.pdf?casa_token=f_wYh5kA57kAAAAA:pG4tYZoMXN_4YNElo3bpW78bwQcQHni052zna1AVq3RYmU934X418ITREIZbJKG8229tiQ by Texas A & M University user on 08 August 2023

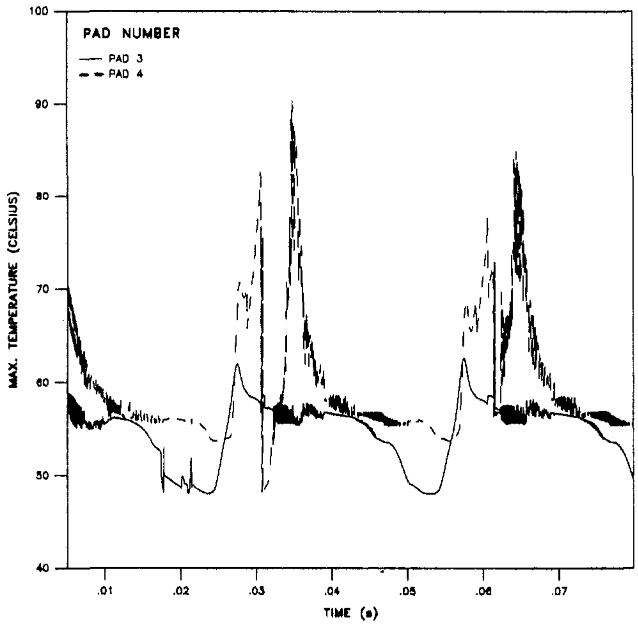

Fig. 12 Maximum film temperature variation with time for high unbalance case ($e_b = 570\ \mu_m$)

film thickness. The IVRP model overpredicts minimum film thickness and therefore may not be adequate. The current research employs a steady state solution of the thermal problem at each time step. Future research will include the exact thermal transient analysis including the $(\partial T/\partial t)$ term and a complete thermoelastohydrodynamic transient analysis of tilt pad journal bearings.

Acknowledgments

The authors wish to thank the Texas A&M University Turbomachinery Research Consortium (TRC) for funding this project.

References

Allaire, P. E., Gunter, E. J., Eierman, R. G., and Nicholas, J. C., 1975, "Film Thickness in Plain Journal, Partial Arc, Axial Groove, Multilobed, Tilting Pad, and Pressure Dam Bearings-A Unified Approach," University of Virginia Report, University of Virginia, Charlottesville, VA.

Choy, F. K., Braun, and M. J., Hu, Y., 1991, "Nonlinear Transient and Frequency Response Analysis of a Hydrodynamic Journal Bearing," ASME Journal of Tribology, Vol. 114, pp. 448-454.

Christie, I., Griffiths, D. F., and Mitchell, A. R, 1976, "The Finite Element Methods for Second Order Differential Equations with Significant First Derivations," *International Journal for Numerical Methods in Engineering*, Vol. 10, pp. 1389-1396.

Earles, L. L., Palazzolo, A. B., and Armentrout, R. W., 1990, "A Finite Element Approach to Pad Flexibility Effects in Tilt Pad Journal Bearings: Parts I and II," ASME Journal of Tribology, Vol. 112, No. 2, pp. 169-182.

Fillon, M., Bligoud, J. C., and Frene, J., 1992, "Experimental Study of Tilting-Pad Journal Bearings-Comparison With Theoretical Thermoelastohydrodynamic Results," ASME Journal of Tribology, Vol. 114, pp. 579-588.

Gadangi, R. K., and Palazzolo, A. B., 1993, "Transient Analysis of Plain and Tilt Pad Journal Bearings Including Fluid Film Temperature Effects," Presented at the ROCON'93, Somerset, NJ, Nov. 10-12.

Huebner, K. H., 1981, *The Finite Element Method for Engineers*, Wiley, New York, NY.

Kim, J., 1992, "Thermoelastohydrodynamic Tilt Pad Journal Bearing Simulation and Application to Rotor-Bearing Model," Ph.D dissertation, Texas A&M University, College Station, TX 77843.

Kim, J., and Palazzolo, A. B., 1993, "Dynamic Characteristics of TEHD Tilt Pad Journal Bearing Simulation Including Multiple Pad Flexibility Model," Presented at the 14th ASME Biennial Conference of Noise and Vibration, Albuquerque, NM.

Malik, M., and Bhargava, S. K., 1992, "Transient Response Investigation of Short Journal Bearing Systems With Flexible Rotors and Damped Flexible Supports," *Tribology Transactions*, Vol. 35, pp. 339-345.

Myrick, S. T., 1973, "Transient and Steady State Response of Flexible Rotor: Real Hydrodynamic Bearing Systems," Ph.D. dissertation, University of Texas, Austin, TX.

Palazzolo, A. B., and Lin, R. R., et al., 1989, "Active Control of Transient Rotordynamic Vibration by Optimal Control Methods," ASME *Journal of Engineering for Gas Turbines and Power*, Apr., Vol. 111, pp. 264-270.

Downloaded from http://asmedigitalcollection.asme.org/tribology/article-pdf/117/2/302/5938013/302_1.pdf?casa_token=f_wYh5kA57kAAAAA:pG4tYZoMXN_4YNElo3bpW78bwQcQHni052zna1AVq3RYmU934X418lITREIZbJKG8229tiQ by Texas A & M University user on 08 August 2023